

Molecular Weight Effects on the Liquid-Crystalline Properties of Poly(vinyl ether)s with Pendant Cyanobiphenyl Mesogenic Groups

Toshihiro Sagane[†] and Robert W. Lenz*

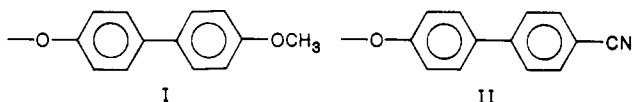
Polymer Science and Engineering Department, University of Massachusetts, Amherst, Massachusetts 01003. Received September 2, 1988;
Revised Manuscript Received February 22, 1989

ABSTRACT: A vinyl ether monomer containing a cyanobiphenyl group, 2-((4'-cyano-4-biphenyl)oxy)ethyl vinyl ether (CBPVE), was cationically polymerized with the hydrogen iodide/iodine (HI/I₂) initiator system and with the hydrogen iodide/zinc iodide (HI/ZnI₂) initiator system to form narrow molecular weight distribution (MWD) polymers. Both of these initiators have been shown to yield "living polymer" polymerization reactions. The thermal properties of poly(CBPVE) were determined by DSC and by observation of samples placed on a hot stage on a polarizing light microscope. Polymer samples which had \bar{M}_n values less than 2600 and a narrow MWD ($\bar{M}_w/\bar{M}_n = 1.02-1.1$) showed enantiotropic liquid-crystalline behavior and formed a smectic phase after one heating cycle. In contrast, the polymer samples having \bar{M}_n values greater than 2600 and a reasonably narrow MWD ($\bar{M}_w/\bar{M}_n = 1.2-1.3$) prepared with these initiators, and also polymers prepared with a boron trifluoride etherate (BF₃OEt₂) initiator which had a broad MWD ($\bar{M}_w/\bar{M}_n = 2.1$, $\bar{M}_n = 4400$), formed only isotropic melts. These molecular weight effects on the thermal properties of poly(CBPVE) are discussed.

Introduction

Side-chain liquid-crystalline polymers, LCP, are of interest for a variety of applications, especially in the field of electrooptics.¹ Although it has been long known that molecular weight and molecular weight distribution are important factors that affect the thermal properties of LCP,² there have been very few reports on this effect.

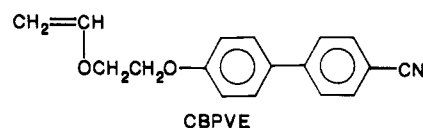
Our previous report described the differences in thermal properties of LCP with both narrow and broad molecular weight distributions, MWDs, which were prepared from 2-((4'-methoxy-4-biphenyl)oxy)ethyl vinyl ether by a living cationic polymerization reaction.³ In that report, we described the properties of a poly(vinyl ether) with a mesogen (I) having an electron-donating group, the methoxy group (OCH₃), at the terminal position of the side chain. In the present study, we prepared a polymer with a mesogen (II) having an electron-withdrawing group, the cyano group (CN), at the terminal position.



Cyanobiphenyl-containing low molecular weight LC compounds are used for display devices, so their LC properties have been thoroughly studied. It is known that the highly polar cyano group attached to one end of the biphenyl group causes the formation of an antiparallel, near-neighbor pairing.^{4,5} It is of interest, therefore, to find out what occurs when a mesogen (II) with a cyano group at its terminal position is attached to a polymer backbone as a side chain. In that type of structure, it may be less likely to form the antiparallel pairing and more likely to show a normal smectic ordering.⁴ Moreover, from our previous work, it will be important to determine if the phase-transition phenomena of the cyanobiphenyl group containing polymers are also effected by their molecular weight distribution.

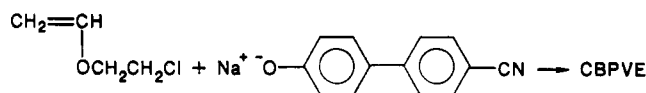
For this purpose, a series of poly(vinyl ether)s containing a pendant cyanobiphenyl group but having different MWDs were prepared by both a living cationic polymerization reaction and a normal cationic polymerization re-

action of 2-((4'-cyano-4-biphenyl)oxy)ethyl vinyl ether (CBPVE). The thermal properties of the polymers so formed were examined in relation to their molecular weights and MWD.



Experimental Section

Materials. 2-((4'-Cyano-4-biphenyl)oxy)ethyl vinyl ether (CBPVE) was prepared by the phase-transfer-catalyzed condensation of 2-chloroethyl vinyl ether with the sodium salt of 4-(4-cyanophenyl)phenol in the presence of a catalytic amount of tetrabutylammonium hydrogen sulfate,⁶ as shown below:



CBPVE was purified by recrystallization from methanol, mp 105 °C (by DSC). The hydrogen iodide (HI), iodine (I₂), zinc iodide (ZnI₂), and boron trifluoride etherate (BF₃OEt₂) initiators and the solvents (methylene chloride, *n*-hexane, and diethyl ether) were purified and used as previously reported.^{7,8}

Polymerization Procedures. Cationic polymerization reactions were carried out as previously reported.^{3,8,9} All polymers were purified by precipitation from CH₂Cl₂ solutions into methanol and were dried under vacuum.

Fractionation and Blending Procedures. Fractionation of polymer B of Table II and Figure 7 was carried out using a methanol/acetone (2/1 v/v%) mixture solvent at room temperature at a concentration of 100 mg of polymer in 10 mL of solvent. The insoluble fraction, designated B-H, was recovered by filtration, and the soluble fraction, B-L, was recovered by evaporation of the solvent.

For the preparation of polymer blends, the two polymers were dissolved in methylene chloride at room temperature at a concentration of 100 mg of total polymer in 10 mL of solvent. In this manner, blends of polymers B and D of Table II and Figure 7 were prepared. The polymer blend was recovered by precipitation from solution into methanol and dried under vacuum before characterization.

Characterization of Monomers and Polymers. The molecular weight distribution of the polymer was measured by GPC in CHCl₃ on a Waters Associates, Inc., liquid chromatograph equipped with five polystyrene gel columns (8 mm × 23 cm each) and a refractive index (RI) detector. The number-average molecular weight (\bar{M}_n) and weight-average molecular weight (\bar{M}_w) were calculated with the use of a polystyrene calibration curve.

[†] Present address: Iwakuni Polymer Research Laboratory, Mitsui Petrochemical Industries, Ltd., Waki-cho, Kuga-gun, Yamaguchi-ken, 740 Japan.

Table III
Thermal Properties of CBPVE Polymers

thermal transitions, °C								
polymer	10 ⁻⁵ \overline{M}_n	$\overline{M}_w/\overline{M}_n$	heating cycle ^a		cooling cycle ^b		thermodynamic params ^c	
			T_g	T_{s-i}	T_{i-s}	T_g	ΔH_{s-i} , cal/g	10 ² ΔS_{s-2} , cal/(g K)
A	1.3	1.04	60 ^e	(115) ^d	96	<i>e</i>	8.1	2.1
B	2.1	1.1	59 ^e	(116) ^d	97	<i>e</i>	5.1	1.3
C	3.5	1.2	72 (57)			66		
D	7.3	1.2	78 (72)			65		
E	4.4	2.1	83 (77)			76		

^a Taken from the first DSC heating cycle; numbers in parentheses indicate the transition temperatures taken from the second heating cycle. ^b Taken from the first DSC cooling cycle. ^c Taken from the second DSC heating cycle. ^d A broad unknown peak from 100 to 180 °C was observed. ^e T_g may overlap with T_{s-i} or T_{i-s} ; see text.

Thermal Properties of Polymers. Typical DSC thermograms for the polymers obtained by HI/I₂, polymers B and C, and by BF₃OEt₂, polymer E, are shown in Figure 2. The HI/I₂-initiated polymer with a low molecular weight and a narrow molecular weight distribution, polymer B, showed a glass transition at 59 °C and a broad endothermic peak from 100 to 180 °C in the first heating cycle. An exothermic transition peak, T_1 , at 96 °C in the first cooling cycle and an endothermic transition peak, T_2 , at 115 °C in the second heating cycle were also observed. The DSC thermogram for polymer A was essentially identical with that of polymer B.

In contrast, the HI/I₂-initiated polymer, C, which has a somewhat higher molecular weight than that of B but also had a narrow MWD, and the BF₃OEt₂-initiated polymer, E, also with a somewhat higher molecular weight but with a broad MWD, showed only a glass transition but not an endotherm. The T_g of polymer C was 57 °C and that of polymer E was 77 °C in their second heating cycles, but unlike polymer B, neither polymer showed either an endothermic peak in any heating cycle or an exotherm peak in any cooling cycle at 10 °C/min. After the first heating cycle, subsequent cycles for each polymer gave virtually identical DSC thermograms.

The thermal transition data and the calculated thermodynamic parameters for all polymers are summarized in Table III. To determine if there was any effect caused by the cooling rate on the thermal properties, a slow cooling rate of 1.25 °C/min was also carried out for polymers C, D, and E. However, no transition peaks were observed for these three polymers, and their thermograms were identical with those obtained at the higher scanning rate.

To identify the broad endothermic peak observed in the first heating cycle, the exothermic transition peak, T_1 , of the first cooling cycle, and the endothermic transition peak, T_2 , of the second heating cycle, texture observations of polymers A and B were made on samples placed on a hot stage of a polarizing microscope. Polymers A and B showed both threadlike textures and dark regions, indicative of the coexistence of a nematic phase and an isotropic phase, above their T_g in the first heating cycle, as shown in Figure 3, with an isotropization temperature at about 150 °C. The fan-shaped textures, which are characteristic of a smectic phase, were observed at a temperature just below T_1 in the cooling cycle, as shown in Figure 4. In contrast, polymers C, D, and E showed no texture, and even after the sample close to T_g in the cooling cycle was annealed for 12 h, no birefringence was observed.

These observations indicate that the broad transition peak in the first heating cycle of polymers A and B, as obtained directly by precipitation from their solution, can be considered to be a transition from the nematic to the isotropic state. Subsequently, the transitions represented by peaks T_1 and T_2 are assigned to the phase transition

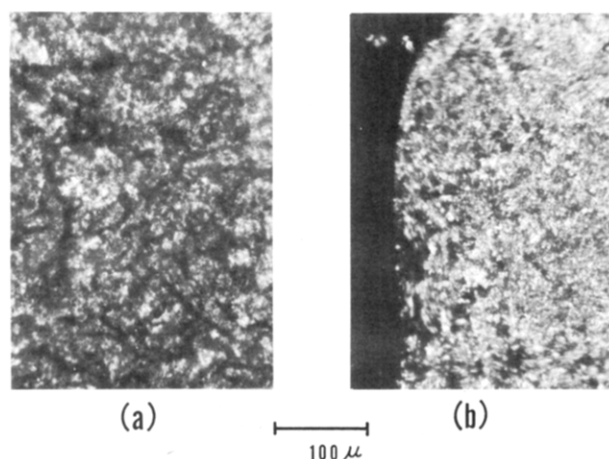


Figure 3. Photomicrograph of the nematic threadlike texture shown by polymer B in the first heating cycle (a) at 75 °C and (b) at 95 °C; at these temperatures, both are above T_g . Magnification is 128×.

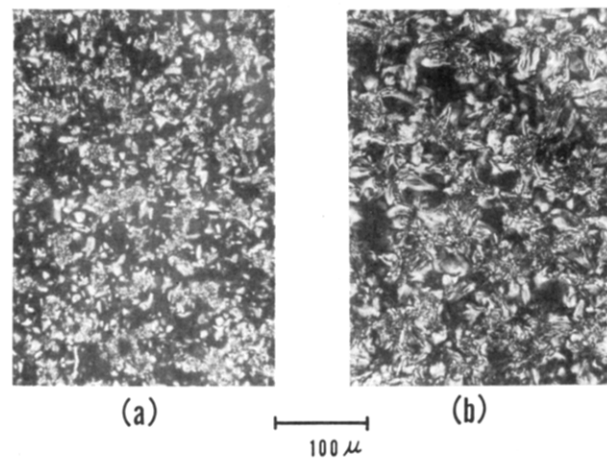


Figure 4. Photomicrographs of the smectic textures shown by the CBPVE polymer obtained by initiation with HI/I₂, polymer B in Table II, in the first cooling cycle: (a) at 90 °C, just below the T_{i-s} , batonnets with focal-conic texture, and (b) after 10 min at the same temperature, focal-conic texture. Magnification is 128×.

from the isotropic state to the smectic (T_{i-s}) state and from the smectic state back to isotropic liquid (T_{s-i}), respectively. A related compound containing the cyanobiphenyl mesogen II, 4-(*n*-octyloxy)-4'-cyanobiphenyl, n,⁴ and a related polymer, the polyacrylate having mesogen II,⁵ were both reported to show the smectic phase too.

Further observations of the textures of polymers A and B in thin-film samples revealed that the phase below T_1 in the first cooling cycle and below T_2 in the second heating cycle is the smectic C phase. This conclusion is based on the fact that the smectic C schlieren texture has point

Table IV
Thermal Properties of CBPVE Polymers after Fractionation and after Blending

sample	$10^{-3}\overline{M}_n^d$	$\overline{M}_w/\overline{M}_n$	thermal transitions (°C) by DSC				thermodynamic params ^g	
			heating cycle ^e		cooling cycle ^f			
			T_g	T_{s-i}	T_{i-s}	T_g	ΔH_{s-i} , cal/g	$10^2\Delta S_{s-i}$, cal/(g K)
B-L ^a	2.1	1.02	58 ⁱ	(106) ^h	90	<i>i</i>	4.9	1.3
B-H ^b	2.6	1.03	67 ⁱ	(111) ^h	85	<i>i</i>	3.5	0.9
F ^c	2.6	1.3	75 (63)			65		

^aLow molecular weight fraction of polymer B. ^bHigh molecular weight fraction of polymer B. ^cBlend of 75% polymer B with 25 wt % polymer D. ^dDetermined by GPC relative to polystyrene standards. ^eTaken from the first DSC heating cycle; numbers in parentheses indicate the transition temperatures taken from the second heating cycle. ^fTaken from the first DSC cooling cycle. ^gTaken from the second heating cycle. ^hA broad unknown peak from 100 to 200 °C was observed. ⁱ T_g may overlap with T_{s-i} or T_{i-s} ; see text.

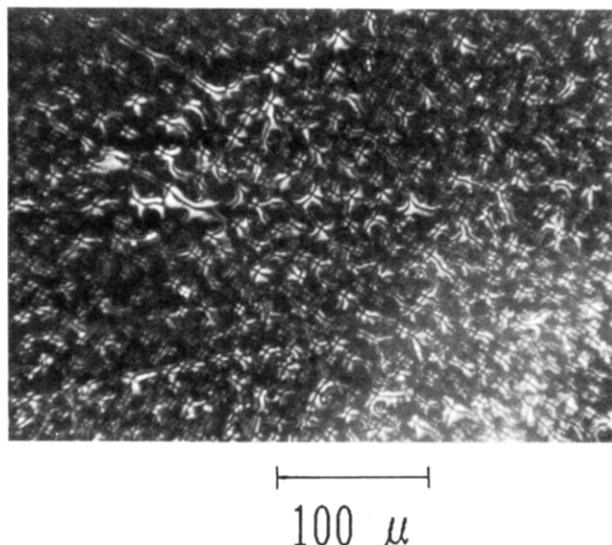


Figure 5. Smectic C schlieren textures shown by polymer B in the first cooling cycle at 96 °C, close to T_{i-s} . Magnification is 128×.

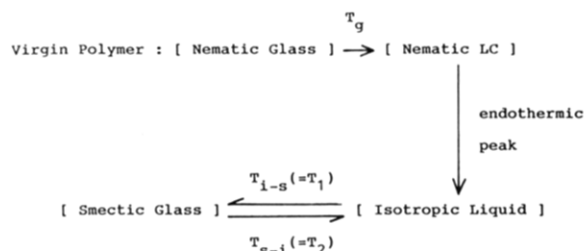
defects with only four brushes ($s = \pm 1$),¹¹ and this texture is seen for polymer B in Figure 5. In contrast, the smectic A phase does not show a schlieren texture.

The virgin samples of polymers A and B showed a T_g transition in the first heating cycles, but neither showed a T_g in subsequent cooling and heating cycles, most likely because their T_g transitions overlapped either the $T_1(T_{i-s})$ or $T_2(T_{s-i})$ transition after the first heating cycle, as was previously observed for LC polymers from 2-((4'-methoxy-4-biphenyl)oxy)ethyl vinyl ether.³ That is, the T_g transition of the smectic glass appears to be higher than that of the nematic glass of the virgin polymer.

The phase transitions of both low and high molecular weight poly(CBPVE)s are summarized in Figure 6. For low molecular weight polymers A and B, the virgin polymers appeared to exist at least partially as a nematic glass, but after one heating cycle through the T_g into the isotropic liquid state and subsequent cooling, they formed the more ordered smectic phase, which was then frozen at the T_g transition; that is, the nematic state becomes monotropic relative to the T_g of the smectic state.³ In that manner, the LC properties of poly(CBPVE) after the first heating cycle were dependent on the molecular weight (MW) and MWD because the lower MW and narrower MWD polymers, polymers A and B, had an accessible transition from the smectic to the isotropic states while the higher MW and broader MWD polymers, polymers C, D, and E, had their T_g above the isotropic to smectic transition temperature. Hence, the latter polymers formed only an amorphous glass on cooling from the isotropic liquid as shown in Figure 6.

Molecular Weight Dependency of the Thermal Properties. In order to reconfirm this interpretation that

Polymers A and B: low MW and narrow MWD polymers



Polymers C, D, and E: high MW and broad MWD polymers

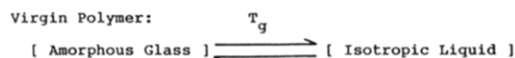


Figure 6. Schematic representation of phase transitions for the different CBPVE polymers.

the relatively lower MW and narrower MWD poly(CBPVE) could show a smectic phase while the relatively higher MW polymer could form only an isotropic phase after the first heating cycle, two experiments were carried out, including (1) fractionation of the broader MWD polymer and (2) blending of the broader and narrower MWD polymers as follows:

(1) Fractionation. Because both polymers A and B contain small amounts of very low MW fractions, this fraction could show a plasticizing effect, which could explain why the overall T_g was depressed and the smectic phase would form. For this reason, the fractionation of polymer B to high and low MW components was carried out, and the thermal properties of each fraction were determined.

(2) Blending. Because the thermal properties of polymers B and C in Table III differed so greatly with increasing \overline{M}_n from 2100 to 3500, then by adding a small amount of the higher MW polymer, which does not show a smectic phase, to the lower MW polymer, which does, it should be possible to change the thermal properties of the latter. Therefore, the thermal properties of a blend of these two polymers were determined.

Figure 7 shows the MWD of the CBPVE polymers before and after fractionation and blending, and the thermal properties of these samples are summarized in Table IV. Two conclusions can be drawn from the data in Table IV: (1) both the higher MW and the lower MW portions of polymer B exhibited a smectic phase, so the reason that polymer B forms a smectic phase cannot be attributed only to the presence of the low MW portion of the sample; (2) by adding only 25% by weight of the higher MW polymer, polymer D, which did not show any mesophase, to the lower MW polymer, polymer B, which did, the thermal properties of B were changed dramatically, and the

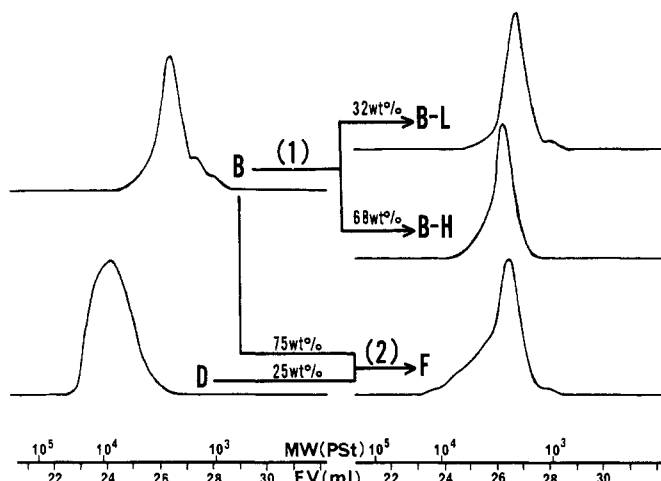


Figure 7. Molecular weight distribution of CBPVE polymers before and after (1) fractionation and (2) blending.

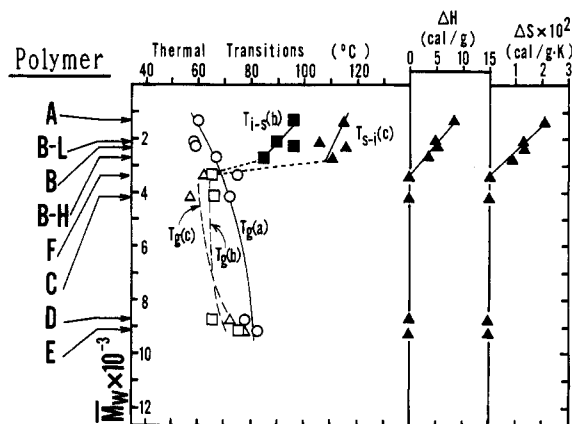


Figure 8. Thermal transition temperatures determined by DSC and thermodynamic parameters, ΔH and ΔS , for the smectic to isotropic transition as a function of \bar{M}_w . Designations are as follows: (a) first DSC heating cycle, (○) T_g ; (b) first cooling cycle, (□) T_g , (■) T_{i-s} ; (c) second heating cycle, (Δ) T_g , (▲) T_{s-i} .

properties of the blend were dominated by that of the higher MW polymer.

The thermal properties of poly(CBPVE) as a function of \bar{M}_w are summarized in Figure 8. Because \bar{M}_w is particularly sensitive to the higher MW portion, this property is an appropriate one to use to discuss the MW dependency of the properties of this polymer.

As shown in Figure 8, polymers having a \bar{M}_w of less than about 3000 showed the transitions between smectic glass

and isotropic liquid after one heating cycle, while polymers having \bar{M}_w of more than about 3000 showed only an amorphous phase, and for the former, the higher the MW of the sample the smaller was the value of ΔH and ΔS (from the smectic phase to the isotropic phase). Furthermore, and very surprising, it is not only the case that T_g increases with increasing MW but also T_{i-s} and T_{s-i} decrease with increasing MW, as depicted in Figure 8. Therefore, the difference between T_g and T_{i-s} also decreases with increasing MW until T_g either increases above T_{i-s} or overlaps with T_{i-s} in some MW range, apparently around a \bar{M}_n value of 3000. As a result, during the cooling cycle, the higher MW polymer became immobile before it rearranged to form the smectic phase.

Acknowledgment. The authors are grateful to the National Science Foundation for the partial support of this work under NSF Grant DMR-8317949 and to Mitsui Petrochemical Industries, Ltd. (Japan), for the support of Toshihiro Sagane. The donation of 4-(4-cyanophenyl)-phenol by Dr. R. A. Willingham and Dr. R. E. Singler of the U.S. Army Material Technology Laboratory is gratefully acknowledged.

Registry No. CBPVE (homopolymer), 120638-02-0; CBPVE, 120638-01-9; $\text{CH}_2=\text{CH}_2\text{OCH}_2\text{CH}_2\text{Cl}$, 110-75-8; HI, 10034-85-2; ZnI_2 , 10139-47-6; I_2 , 7553-56-2; BF_3OEt_2 , 109-63-7; sodium 4-(4-cyanophenyl)phenoxide, 119303-21-8.

References and Notes

- (1) (a) Finkelmann, H.; Keichle, U.; and Rehage, G. *Mol. Cryst. Liq. Cryst.* 1983, 94, 343. (b) Coles, H. J.; Simon, R. In *Recent Advances in Liquid Crystalline Polymers*, Chapoy, L. L., Ed.; Elsevier Applied Science, New York, 1985; Chapter 22.
- (2) Finkelmann, H. In *Polymer Liquid Crystals*; Ciferri, A., Krinbaum, W. R., Meyer, R. B., Eds.; Academic Press: New York, 1982; Chapter 2.
- (3) Sagane, T.; Lenz, R. W. *Polym. J.* 1988, 20, 923.
- (4) Gray, G. W. In *Polymer Liquid Crystals*; Ciferri, A.; Krinbaum, W. R., Meyer, R. B., Eds.; Academic Press: New York, 1982; Chapter 1.
- (5) Barny, P. L.; Dubois, J.-C.; Friedrich, C.; Noel, C. *Polym. Bull.* 1986, 15, 341.
- (6) Rodriguez-Parada, J. M.; Percec, V. *J. Polym. Sci., Polym. Chem. Ed.* 1986, 24, 1363.
- (7) (a) Miyamoto, M.; Sawamoto, M.; Higashimura, T. *Macromolecules* 1984, 17, 265; (b) 1984, 17, 2228.
- (8) Sawamoto, M.; Okamoto, C.; Higashimura, T. *Macromolecules* 1987, 20, 2693.
- (9) Enoki, T.; Sawamoto, M.; Higashimura, T. *J. Polym. Sci., Polym. Chem. Ed.* 1986, 24, 2261.
- (10) (a) Aoshima, S.; Hasegawa, O.; Higashimura, T. *Polym. Bull.* 1985, 13, 229; (b) 1985, 14, 417. (c) Nakamura, T.; Aoshima, S.; Higashimura, T. *Polym. Bull.* 1985, 14, 515. (d) Choi, W. O.; Sawamoto, M.; Higashimura, T. *Polym. J.* 1987, 19, 889.
- (11) Demus, D.; Richter, L. *Textures of Liquid Crystals*; Verlag Chemie: New York, 1978.